IOP Conf. Series: Materials Science and Engineering **232** (2017) 012020 doi:10.1088/1757-899X/232/1/012020

CFD simulation of a screw compressor with oil injection

Hui Ding, and Yu Jiang

Simerics Inc.,
1750 112th Ave NE Ste C250,
Bellevue, WA 98004, USA

E-mail: hd@simerics.com

Abstract. In this paper, a full 3D transient CFD model of a twin screw compressor with oil injection will be described in detail. The Volume Of Fraction (VOF) approach was used for two phase flow of gas and liquid. The numeric method and simulation conditions will be explained. Simulation results will be presented with discussion. The cooling and sealing effects of oil injection will be evaluated by comparing the simulation results for the cases with and without oil. The imbalance of mass and energy of the compression system in simulation results will be rigorously checked to prove the methodologies used in the simulation are fully conservative and consistent. The efficiency, speed, and robustness of the proposed approach will also be demonstrated through the test case.

1. Introduction

Besides lubricating the gears, oil injection has been commonly used in different types of positive displacement compressors to cool the compressed gases and to seal the leakage gaps to improve compressor gas flow rate and efficiency [1]. CFD simulation provides valuable insights to help compressor designers to verify, to analyze, and to improve the performance of compressors. It is very beneficial if CFD can be applied to the analysis of compressors with oil injection.

In recent years, CFD has been widely used to analyze performance of varies Positive Displacement (PD) compressors. Those models cover different types of PD compressors with/without intake and/or discharge valves but mostly solving single gas phase flow.

Solving two phase flow using CFD with complex moving parts and small leakage gaps is a very challenging task. Even for relatively simple two-phase flow problems, high density ratio between liquid and gas, sophisticated interaction among the phases, and the interface tracking with complex shape make the problem difficult to solve. It is even more difficult to solve a multiphase flow in a PD compressor. In such case, gas phase has to be treated as compressible, heat transfer effects has to be included, and interface tracking has to be done inside moving, deforming volumes. The major issues users have experienced with many CFD solvers in multiphase simulations are poor convergence, very long simulation time, and unsatisfactory mass/energy conservation. Generally speaking, CFD simulation of compressors with liquid injection is a very difficult task.

As a test case for Simerics improved VOF model, Ding and Jiang (2016)[2] has used Simerics-MP+ (also known as PumpLinx) solved an oil flooded scroll compressor. In the study, the oil was assumed to be uniformly mixed with the gas at the compressor inlet with up to 18% oil mass fraction. The simulation results demonstrated good convergence, fast calculation speed, and excellent conservation of mass and energy. However, the simulated conditions are relatively ideal.

In this paper, a screw compressor with oil injection is investigated using VOF model. Compared with previous work by Ding and Jiang [2], this study uses a more realistic model with much higher oil mass fraction of up to 57%. In the following sections, the proposed CFD model of the screw compressor with oil injection will be described in detail. Simulation results will be presented and discussed. The conservation of mass and energy as well as the flow and thermodynamic cycles inside the compression chamber will be subtracted from simulation results. The overall oil injection effects on the compressor performance will be evaluated by comparing the simulation results with/without oil injection.

2. CFD solver and governing equations

2.1. Conservation equations for gas liquid mixture

The CFD package, Simerics-MP+, used in this study solves conservation equations of mass, momentum, and energy of a compressible fluid using a finite volume approach. Those conservation laws can be written in integral representation as

$$\frac{\partial}{\partial t}\int_{\Omega(t)} \rho d\Omega + \int_{\sigma} \rho(\mathrm{v}-\mathrm{v}_{\sigma})\cdot \mathrm{n} d\sigma = 0 \tag{1}$$

$$\frac{\partial}{\partial t}\int_{\Omega(t)} \rho \boldsymbol{v} d\Omega + \int_{\sigma} \rho\big((\boldsymbol{v}-\boldsymbol{v}_{\sigma})\cdot \boldsymbol{n}\big)\boldsymbol{v} d\sigma = \int_{\sigma} \tilde{\boldsymbol{\tau}}\cdot \boldsymbol{n} d\sigma - \int_{\sigma} p\boldsymbol{n} d\sigma + \int_{\Omega} f d\Omega \tag{2}$$

$$\frac{\partial}{\partial t}\int_{\Omega(t)} \rho E d\Omega + \int_{\sigma} \rho\big((\boldsymbol{v}-\boldsymbol{v}_{\sigma})\cdot \boldsymbol{n}\big)E d\sigma = \int_{\sigma} k\nabla T\cdot \boldsymbol{n} d\sigma - \int_{\sigma} p\boldsymbol{v}\cdot \boldsymbol{n} d\sigma + \int_{\sigma} (\boldsymbol{v}\cdot\tilde{\boldsymbol{\tau}})\cdot \boldsymbol{n} d\sigma + \int_{\Omega} \boldsymbol{f}\cdot \boldsymbol{v} d\Omega \tag{3}$$

The standard $k-\varepsilon$ two-equation model [3] with wall function is used to account for turbulence,

$$\frac{\partial}{\partial t}\int_{\Omega(t)} \rho k d\Omega + \int_{\sigma} \rho\big((\boldsymbol{v}-\boldsymbol{v}_{\sigma})\cdot \boldsymbol{n}\big)k d\sigma = \int_{\sigma} (\mu+\frac{\mu_t}{\sigma_k})(\nabla k\cdot \boldsymbol{n}) d\sigma + \int_{\Omega} (G_t - \rho\epsilon) d\Omega \tag{4}$$

$$\frac{\partial}{\partial t}\int_{\Omega(t)} \rho \varepsilon d\Omega + \int_{\sigma} \rho\big((\boldsymbol{v}-\boldsymbol{v}_{\sigma})\cdot \boldsymbol{n}\big)\varepsilon\, d\sigma = \int_{\sigma} (\mu+\frac{\mu_t}{\sigma_\varepsilon})(\nabla\epsilon\cdot \boldsymbol{n}) d\sigma + \int_{\Omega} (c_1 G_t\frac{\varepsilon}{k} - c_2\rho\frac{\varepsilon^2}{k}) d\Omega \tag{5}$$

Together with equation of state, where properties are functions of temperature and pressure, to form a closed system:

$$\rho = f(p,T) \tag{6}$$

In the solver, each of the fluid properties will be a function of local pressure and temperature, and can be prescribed as an analytical formula or in a table format.

2.2. VOF model for multiphase

VOF models are widely used in simulation of two phase flow [4] [5]. VOF solves a set of scalar transport equations representing the volume fraction of each fluid component occupies in every computational cell. The transport equation of the volume fraction for each fluid component can be written as:

$$\frac{\partial}{\partial t}\int_{\Omega(t)} \rho_i F_i d\Omega + \int_{\sigma} \rho_i(\mathrm{v}-\mathrm{v}_{\sigma})\cdot \mathrm{n} F_i d\sigma = 0 \tag{7}$$

Where F_i is the volume fraction of the *ith* fluid component, and ρ_i is the local density of *ith* fluid component. The weighted mixture density of the fluid in equation (1) to (5) are then calculated as:

$$\rho = \sum \rho_i F_i \tag{8}$$

Both implicit and explicit methods can be used to solve the equation. High Resolution Interface Capturing (HRIC) scheme can be used for the convective term in the transport equation.

IOP Conf. Series: Materials Science and Engineering **232** (2017) 012020 doi:10.1088/1757-899X/232/1/012020

This software package has been validated against many different types of compressors including: centrifugal compressor, lobe compressor, twin screw compressor [6], scroll compressor [7] [8], rolling piston [9], and reciprocating compressor [10] for single phase compression of air, refrigerants, and other type of gases. The VOF model has also been validated against many industrial applications for multiphase flow without solving heat transfer directly [11] [12], and for multiphase flow solving together with heat transfer [2].

3. Twin screw compressor test case

The compressor model used in this study was originally designed as an oil-free twin screw compressor with a 3/5 lobe arrangement and 'N'rotor profile rotors [6]. The operating speed on the male rotor varies from 6000 to 14000 rpm. The male rotor diameter is 127.45 mm; the female rotor diameter is 120.02 mm while the center distance between the two rotors is 93.00 mm. The length to diameter ratio of the rotors is 1.6 and the male rotor has a wrap angle 285.0 deg. In this study, two oil injection pipes were added to both male and female rotor. The discharge port was also modified in order to generate higher compression ratio, such that the oil cooling becomes important.

The rotor part of the twin screw was meshed as a single domain using a grid generation software SCORG [6]. SCORG creates a series of mesh files for the rotor at different rotation angles. The rotor mesh files were read into the solver through Simerics - SCORG mesh interface. The inlet and outlet ports of fluid volumes are meshed using Simerics binary tree unstructured mesher. All the fluid volumes are connected together using Mis-matched Grid Interface (MGI). The total number of cells is around 0.86 million. Figure 1 and 2 show the complete simulation fluid domain and the mesh in 3D view.

The gas inlet is set to a fixed total pressure, and a fixed total temperature boundary condition while the outlet is set to a fixed static pressure boundary condition. The gas phase of the fluid is air, modelled using ideal gas law. The male rotor rotation speed is 8000 RPM. The oil is assumed to be incompressible with a density of 950 Kg/m3, and a heat capacity of 1670 J/kgK. In order to demonstrate the effects of oil injection, a similar case with the same parameters but without oil was also simulated for comparison. Simulation time is about 4 hours per revolution for the simulation with oil injection and about 2 hours per revolution without oil on a Dell Precision Mobile Workstation with Intel i7-4800MQ CPU @ 2.70GHz.

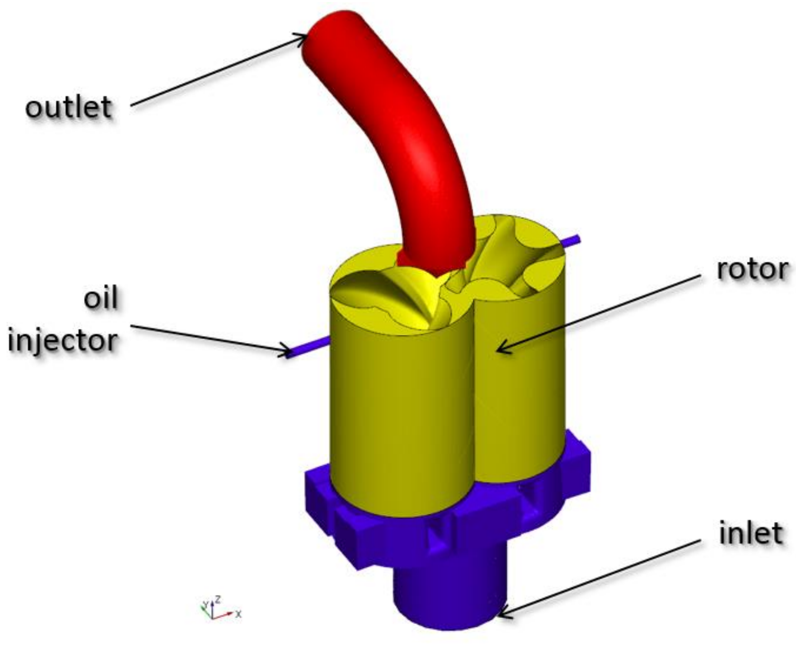

Figure 1: All fluid volumes

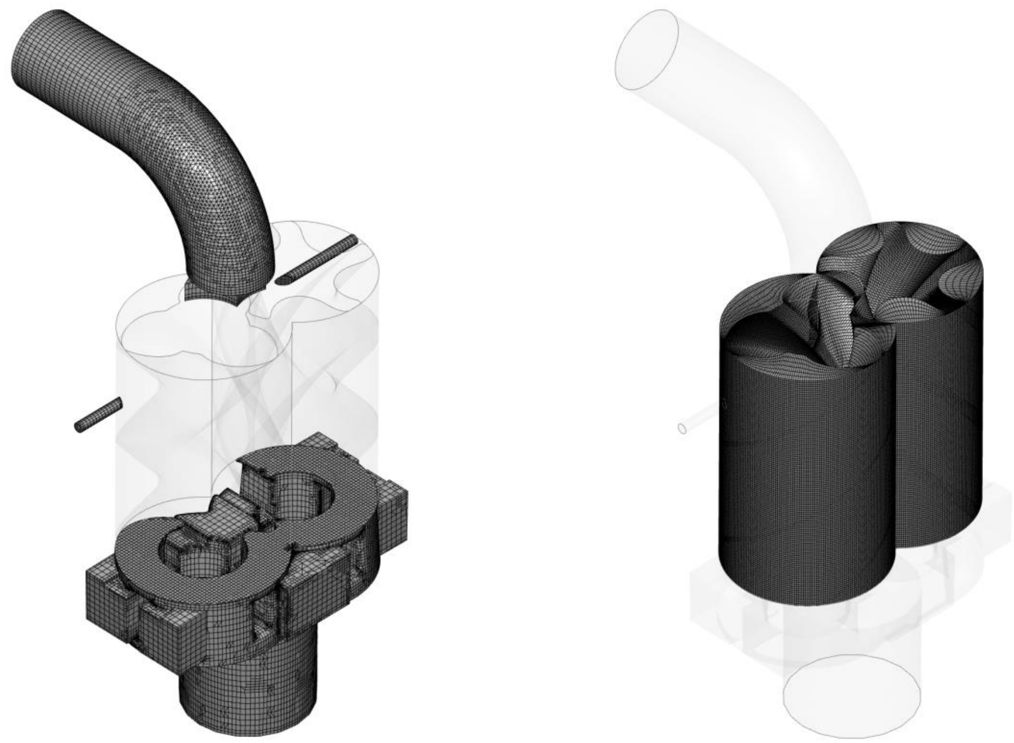

(a) (b)

Figure 2: Mesh: (a) ports mesh (b) rotor mesh

4. Results and discussion

In the simulation, the inlet total pressure and the outlet static pressure are set to 1 atm and 5 bar respectively. The inlet total temperature is set to 300K. The oil is injected from two pipes with 2 gpm flow rate from each pipe and with inlet temperature of 320K. Both rotors are assigned with correct rotational speed. Table 1 summarizes simulation parameters used for the oil injection simulation.

Table 1: Simulation parameters

Parameters	Values
Gas	Air (using ideal gas law)
Gas inlet total pressure	1 atm
Gas inlet total temperature	300 K
Outlet static pressure	5 bar absolute
Oil density	950 kg/m^3
Oil viscosity	0.008 PaS
Oil heat capacity	1670 J/KgK
Oil injection rate	2 x 2 gpm
Oil injection temperature	320 K
Compressor speed	8000 rpm (male rotor)

During the simulation, results become periodic after around 6 revolutions. Figure 3 shows typical pressure contour at 5 different male rotor crankshaft angles for one complete tooth rotation. The colour map ranges from 1 bar to 6.5 bar with magenta represents high pressure and blue represents low pressure. During the operation, isolated fluid "pockets" move up from inlet port to the discharge port. The pressure in each pocket keeps increasing with crankshaft angle due to the continuous volume reduction of the pocket until it reaches outlet.

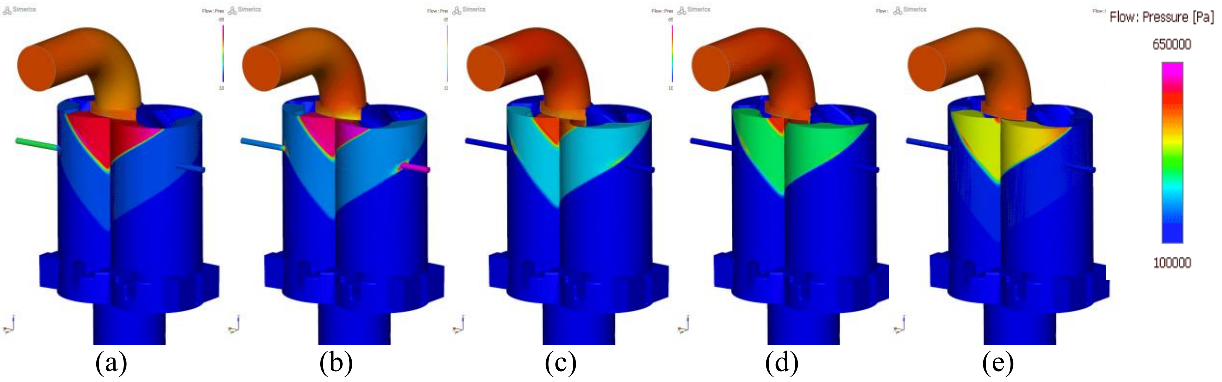

Figure 3: Pressure contour at different male rotor crankshaft angles: (a) 24 degree (b) 48 degree (c) 72 degree (d) 96 degree (e) 120 degree

Figure 4 shows temperature contour at 5 crankshaft angles. The colour map ranges from 300 K to 550 K with magenta represents high temperature and blue represents low temperature. Temperature in the pocket follows a similar trend. However, unlike the pressure, the temperature inside each pocket is highly non-uniform due to the cooling effects of injected oil. The region close to the oil injection has significantly lower temperature.

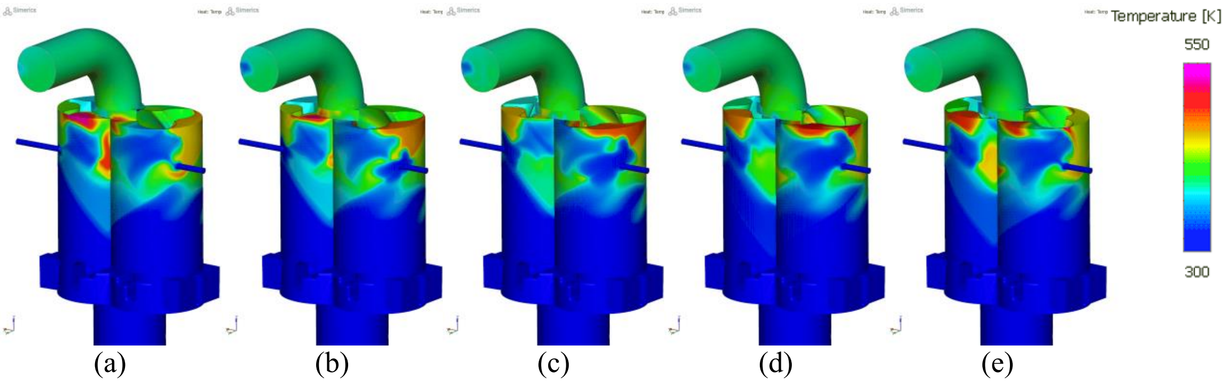

Figure 4: Temperature contour at different male rotor crankshaft angles: (a) 24 degree (b) 48 degree (c) 72 degree (d) 96 degree (e) 120 degree

Figure 5 shows oil concentration contour at 5 crankshaft angles. The colour map ranges from 0% to 10% volume fraction of oil with magenta represents high concentration and blue represents low concentration. Oil has higher concentration close to the injector and then been carried away by the pocket.

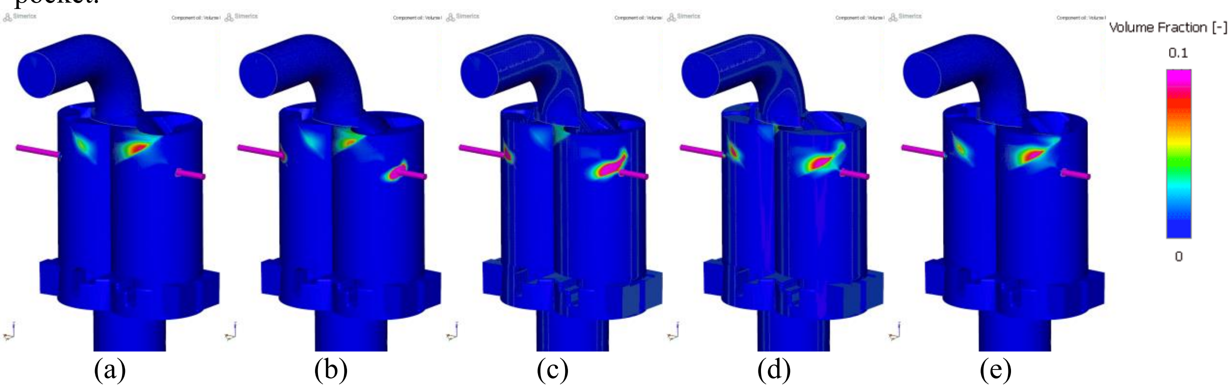

Figure 5: Oil concentration contour at different male rotor crankshaft angles: (a) 24 degree (b) 48 degree (c) 72 degree (d) 96 degree (e) 120 degree

Figure 6 shows oil concentration iso-surface at 5 crankshaft angles with rotor surface coloured by temperature. After injected into the rotor, the oil is not well mixed with the gas. Instead, the oil is still hold together to form very non-uniform concentration in the rotor chamber. Also from the picture, the oil cooling effects are demonstrated clearly as the areas around the oil have significantly lower temperature.

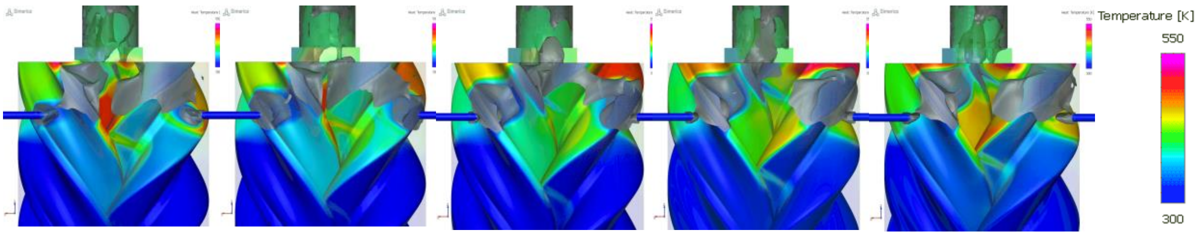

(a) (b) (c) (d) (e)

Figure 6: Oil iso-surface with rotor colored by temperature at different male rotor crankshaft angles: (a) 24 degree (b) 48 degree (c) 72 degree (d) 96 degree (e) 120 degree

For the case with oil injection, the average gas mass flux of the compressor under simulation condition is 0.1794 kg/s. The oil mass fraction, defined as average oil mass flow rate divide by total mass flow rate, is about 57%. The average outlet temperature is about 391 K. Table 2 summarizes mass and energy balances over one male rotor revolution after solution becomes periodic.

Table 2: Mass and energy balance

	Gas inlet	Oil injector	Outlet	Rotor power	Imbalance
Gas mass flow rate (kg/s)	*0.1794*	*0*	*0.1808*	*N/A*	*0.8%*
Oil mass flow rate (kg/s)	*0*	*0.2398*	*0.2385*	*N/A*	*0.5%*
Heat flux/Power (kw)	*53.0*	*128.2*	*226.5*	*46.4*	*0.5%*

Figure 7 plots instantaneous gas flow rate at inlet and outlet vs. male rotor crankshaft angle for two male rotor revolutions after solution becomes periodic. The results show perfect periodic shape repeated for every rotor tooth rotation. Outlet flow rate shows more oscillation than inlet flow rate, and has a short period of reverse flow.

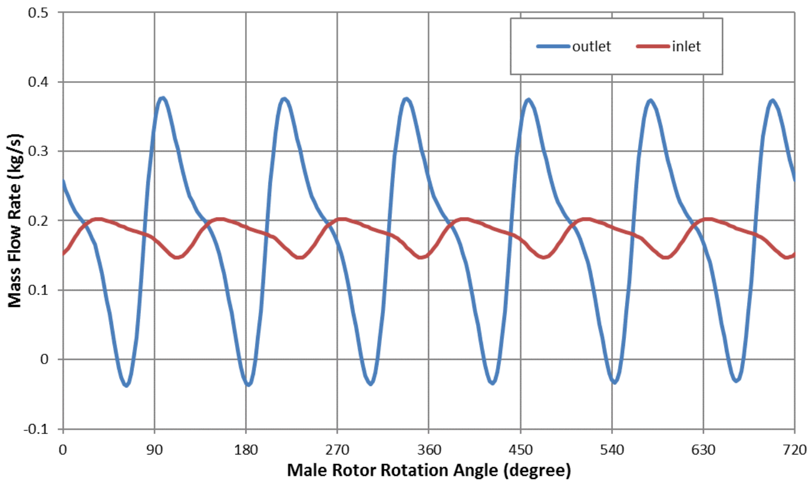

Figure 7. Gas mass flow at inlet and outlet

In order to evaluate oil injection effects on compressor performance, a similar case with the same condition but without oil injection has also been simulated. For the gas only case, the simulation imbalance of gas mass flowrate is about 0.4%, and the energy imbalance is about 0.2%. Figure 8 compares pressure distributions for the case with and without oil at the same crankshaft angle. Although the discharge pressures are the same, the internal pressure for the case without oil is significantly higher than the case with oil. Figure 9 compares temperature distributions for the case with and without oil at the same crankshaft angle. The temperature for the case without oil is much higher than the case with oil.

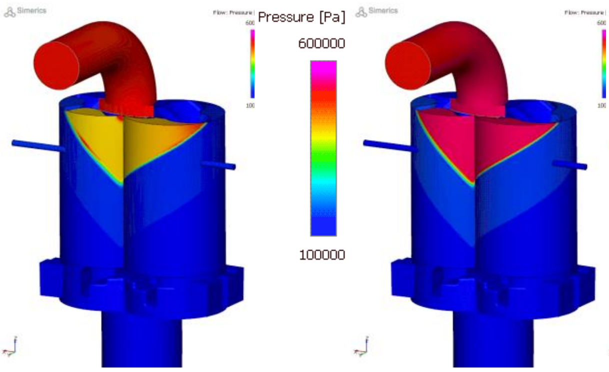

(a) (b)

Figure 8: Comparison of pressure: (a) with oil (b) without oil

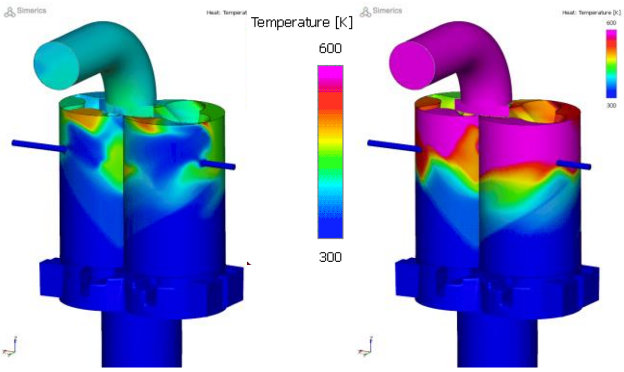

(a) (b)

Figure 9: Comparison of temperature: (a) with oil (b) without oil

Table 3 summarizes differences in compressor performance with/without oil injection. With oil injection, the compressor running under the same condition has a 23% increasing in gas mass flow rate, a 74% reduction of gas temperature rise at outlet, and a 12% reduction in rotor power compared with the "dry" (without oil injection) operation. The performance improvement of compressor with oil injection could be contributed from the combined effects of oil cooling and oil sealing.

Table 3: Effects of oil injection on compressor performance

	Gas mass flow rate (kg/s)	**Gas temperature rise[a] (K)**	**Rotor power (kw)**
With oil injection	0.1808	91	46.4
Gas only	0.1465	353	52.8
Differences	+23%	-74%	-12%

[a] With reference to inlet gas temperature of 300 K.

Figure 10 plots the pressure history of one compression pocket for both cases with and without oil injection for two revolutions of male rotor. The plotted pocket data was obtained from a monitor point moving together with the pocket.

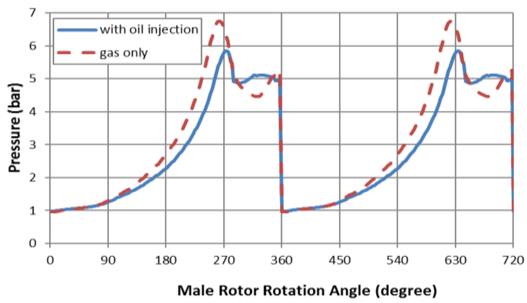

Figure 10: Pressure history of a pocket

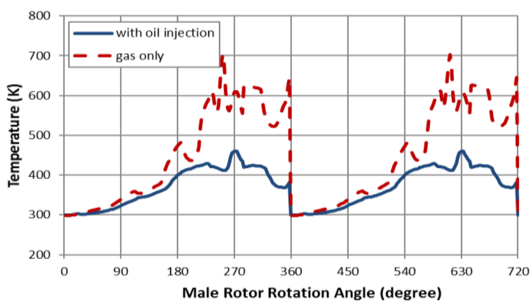

Figure 11: Temperature history of a pocket

The history curves show clear periodic patterns. The case without oil injection has a higher over compression than the one with oil. Figure 11 plots the temperature history of the same pocket. Due to the non-uniformity of the temperature field, the temperature results obtained from the monitor point have much more oscillation than the pressure results. The case without oil has a much higher temperature.

5. Summary

A newly improved VOF multiphase model has been successfully applied to the modelling of a twin screw compressor with oil injection. Simulation results predicted correct trends of performance improvement due to oil injection by comparing with a similar model operating without oil. Simulation results also show excellent mass and energy conservations. Detailed flow patterns and thermodynamic history of compression process with oil injection have been revealed from simulation results, which will help compressor designer and analyst to better understand and to improve the design. Overall, this new model has demonstrated great potential to be a very useful tool for the analysis of two phase flow problems in PD compressors.

Acknowledgement

The authors would like to express our gratitude to Dr. Kovacevic and Dr. Rane of City University London for letting us use their twin screw rotor geometry and mesh in this study.

References

[1] Bell, I., 2011. Theoretical and Experimental Analysis of Liquid Flooded Compression in Scroll Compressors. Ph.D. thesis, Purdue University. Full-text: http://docs.lib.purdue.edu/herrick/2/

[2] Ding, H. and Jiang, Y., "CFD Simulation of An Oil Flooded Scroll Compressor Using VOF Approach" (2016). International Compressor Engineering Conference. Paper 2508

[3] Launder, B.E., and Spalding, D.B., 1974, The numerical computation of turbulent flows, Comput. Methods Appl. Mech. Eng., 3, pp. 269-289.

[4] Ubbink, O., 1977. "Numerical prediction of two fluid systems with sharp interfaces". Ph.D. Thesis, Department of Mechanical Engineering, Imperial College, University of London.

[5] Hirt, C.W. and Nichols, B.D., 1981, Volume of fluid (VOF) method for the dynamics of free boundaries. J. Comput. Phys., Vol. 39, p. 201-225.

[6] Kovacevic, A., Rane, S., Stosic, N., Jiang, Y., and Lowry, S., 2014, Influence of approaches in CFD Solvers on Performance Prediction in Screw Compressors, *Int. Compressor Engrg. Conf. at Purdue*.

[7] Gao, H., and Jiang, Y., 2014, Numerical Simulation of Unsteady Flow in a Scroll Compressor, *Int. Compressor Engrg. Conf. at Purdue*.

[8] Gao H., Ding, H., and Jiang, Y., 2015 "3D Transient CFD Simulation of Scroll Compressors with the Tip Seal,"IOP Conference Series: Materials Science and Engineering. Vol. 90. No. 1. IOP Publishing, 2015.

[9] Ding, H. and Gao, H., 2014,"3-D Transient CFD Model For A Rolling Piston Compressor With A Dynamic Reed Valve", 2014, *22nd International Compressor Engineering Conference*, Paper 1548.

[10] Dhar, S., Ding, H., and Lacerda, J., 2016, "A 3-D Transient CFD Model of a Piston Reciprocating Compressor with Dynamic Port Flip Valves," *23rd Int. Compressor Engrg. Conf. at Purdue*. Paper 1392.

[11] Ding, H., Jiang, Y., Wu, H., and Wang, J., 2015, "Two Phase Flow Simulation of Water Ring Vacuum Pump Using VOF Model," ASME/JSME/KSME 2015 Joint Fluids Engineering Conference, Seoul, South Korea, July 26–31, 2015

[12] Kucinschi, B. and Shieh, T., "Estimation of Oil Supply Time during Engine Start-Up at Very Low Temperatures," SAE Int. J. Fuels Lubr. 9(2):2016, doi:10.4271/2016-01-0893.